

Endoscopic PIV in a helical pipe coil

Franco Auteri, Marco Belan, Sara Ceccon, Giuseppe Gibertini, Maurizio Quadrio

Dipartimento di Ingegneria Aerospaziale
Politecnico di Milano
via La Masa 34, 20156 Milano

ABSTRACT

In recent years curvature effects on the wall turbulence structure have been the subject of an intense research. At present, these topics are being investigated both numerically and experimentally at the Dipartimento di Ingegneria Aerospaziale, Politecnico di Milano.

This work deals with an experimental research project about the properties of the turbulent flow in a helical coil. The facility consists of a reinforced rubber circular duct, filled with water, which is wrapped on a cylindrical core (the core diameter is 10 times the pipe diameter) in such a way that the coils are tightly in touch. An endoscopic PIV system has been developed in order to investigate mean flow and wall turbulence properties on planes both normal and parallel to the duct axis. Suitable endoscopic optical devices for lighting and image acquisition, a continuous Argon Ion Laser 2W green laser and a fast gated image intensifier, are employed. Fluorescent particles and narrow-band optical filters will be used to achieve a better signal-to-noise ratio in the region very close to the wall.

1. Introduction

The study of fluid flow in helically coiled pipes is important both for engineering applications and scientific interest. As evident from the review article by Berger, Talbot and Yao¹, many industrial processes require curved ducts to satisfy space and geometric requirements: heat exchangers, chemical reactors, exhaust gas ducts of engines, evaporators, condensers, storage tanks, piping systems. Flow in curved pipes is also important in bioengineering applications (i.e. blood flow in the human arterial system). From the basic research viewpoint, the study of pipe centerline curvature on flow structures and turbulence is a very interesting subject.

The laminar flow in coiled pipes has been studied in detail and is well understood²⁻⁵. Despite its pervasive interest, however, the turbulent regime remains poorly understood and numerical and experimental investigations are currently conducted to understand transition to turbulence^{6,7} and the fully developed turbulent regime^{8,9}. A main difference between the flow through a helical coil with respect to the flow through a straight pipe is the presence of secondary flows arising from the imbalance between centrifugal force, directed in the outward direction, and pressure force, directed inward, acting on the fluid. These secondary flows consist of counter-rotating structures. Secondary flows in curved ducts are usually called “Dean vortices” by many authors⁹⁻¹¹ but, as shown by Hüttl and Friedrich⁹, no significant pressure minima are observed at the center of these structures, therefore the term vortex may be improper. For this reason in this work the expression “Dean flows” will be used. Secondary flow can influence heat and mass transfer. The curvature of the coil tends to dampen high-frequency turbulent fluctuations, so that a higher value of Reynolds number is necessary to establish a fully developed turbulent flow compared to the straight pipe^{8,12}. Furthermore the point of maximum axial velocity, located in the center of the cross section for a straight pipe, moves outwards, as shown by Berger et al¹.

A coordinated numerical and experimental research project has been planned and the construction of a specific experimental facility is under way at Politecnico di Milano. The aim of this research project is to investigate the turbulent flow in a helical pipe of circular cross-section, and in particular to study the secondary structures in turbulent conditions with a Particle Image Velocimetry (PIV) technique (for details about PIV see Raffel et al¹³ while for an example of endoscopic PIV application see Xiong and Merzkirch¹⁴). In the available literature experimental studies are reported for the helical coil problem based on Laser-Doppler Velocimetry⁶ or flow visualization¹¹, but in the authors knowledge it is the first time an endoscopic technique is used for this kind of flow.

The facility consists of a duct of appropriate geometry with water flow inside. In order to obtain completely developed flow conditions (i.e. no inlet conditions dependency) a coil geometry has been chosen. The pipe coil geometry and flow parameters have been chosen in such a way that the flow will be very similar to the ideal toroidal pipe flow. Due to the particular flow geometry, endoscopic PIV is necessary to visualize and measure the vortical structures in the flow and

therefore a specific system has been set up. The whole experimental system (configuration, materials, instruments, etc...) has been studied and realized from scratch. Therefore in this work we deal with preliminary evaluations and with the choice of the instruments and preliminary tests.

2. The pipe

Referring to Figure 1 we can define the following parameters that completely define the coil geometry:

- the curvature $k = \frac{R_c}{R_c^2 + p_s^2}$,
- the torsion $\tau = \frac{p_s}{R_c^2 + p_s^2}$,
- the torsion to curvature ratio $\lambda = \tau / k$,
- the curvature ratio $\delta = a / R_c$.

For $\lambda = 0$ the helical coil becomes a torus. To conform as much as possible to the toroidal geometry, the torsion to curvature ratio has been kept as low as possible in the present setup, $\lambda \ll 1$.

Other important quantities and parameters are¹⁵⁻¹⁷:

- the bulk velocity U_b ,
- the Reynolds number $Re = 2aU_b/\nu$,
- the Dean number $De = Re\sqrt{\delta}$,
- the Germano number $Gn = \lambda Re$.

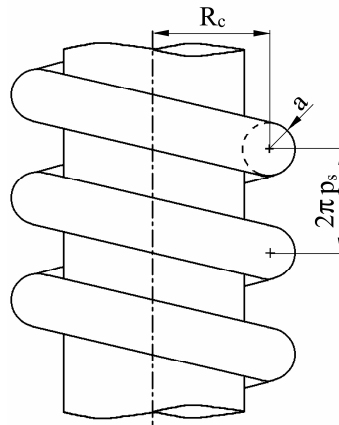


Figure 1. Basic coil dimensions

The present pipe has a coil radius $R_c = 0.509$ m and an internal pipe radius $a = 0.051$ m leading to $\delta = 0.1$. The external pipe diameter is 0.118 m and, as the coil wraps are kept as close as possible as can be seen in Figure 2, this leads to a curvature $k = 1.96$ m⁻¹, a torsion $\tau = 0.0724$ m⁻¹ and finally to a torsion to curvature ratio $\lambda = 0.037$.

According to Srinivisan et al¹² in order to be sure that the flow is fully turbulent the Reynolds number must be

$$Re \geq 2100 \left(1 + 12\sqrt{a/R_c} \right) = 10^4$$

which means that the bulk velocity must be greater than 0.11 m/s.

A Reynolds number equal to 10^4 will produce a Dean number $De = 3.2 \cdot 10^3$ and a Germano number $Gn = 3.7 \cdot 10^{-6}$. The Dean number is large enough and the Germano number is sufficiently small in the present configuration to guarantee that a couple of counter-rotating and essentially symmetric Dean vortices will be present as secondary flow^{6,9}.

Particular attention has to be devoted to imperfections and surface finishing when selecting the duct. Two main possibilities are currently available to build the duct: one is to bend and solder metallic tubes; the other is to bend a plastic tube on a cylindrical core. The first technique allows a better internal surface quality, but for the solder joints that

can be quite near one another (approximately 6 meters). The second technique allows to take rid of joints since tubes as long as 40 m can be produced with current technology, but particular attention must be paid to internal surface finishing. In particular, attention should be paid to surface waves produced by springs that are present in armed tubes to maintain section shape. Such roughly sinusoidal waves on the wall can heavily influence the flow, as shown in a paper by Nakagawa and Hanratty¹⁸, where the influence of a structured wavy wall on turbulence is studied. We can assume the same important influence on a coiled pipe flow, and in particular on the secondary Dean flows. It is reasonable to imagine that a large sinusoidal disturbance can destroy such structures. According to Nakagawa and Hanratty, wall waves with an amplitude lower than 0.5 mm can be accepted for our purposes.

Perfectly smooth walls are considered in numerical Dean flow studies of course, i.e. the roughness of the wall $\varepsilon = 0$. In an experimental work a residual roughness is always present. Literature on roughness effects is rich and not uniform: for example it seems that $\varepsilon^+ = 0.001 \div 5$ is the range of admissible dimensionless roughness if the mean velocity profile in the straight case is considered. Internal surface finishing of the pipe must satisfy this fundamental requisite.

The viscous length δ_v in our case can be computed by

$$\delta_v = \frac{\nu}{u_\tau}$$

where u_τ is the friction velocity and ν is the kinematic viscosity. u_τ can be estimated starting from numerical simulations (see for instance Quadrio and Sibilla¹⁹), which give, for a straight pipe at $Re=4900$ where Re is based on centreline streamwise velocity and pipe radius,

$$\frac{U_b}{u_\tau} \approx 14.$$

Hence:

$$\delta_v = \frac{\nu}{u_\tau} = \frac{1.14 \cdot 10^{-6}}{0.07/14} = 0.023 \text{ mm}$$

A pipe with roughness less than $\varepsilon = 0.02$ mm, which means $\varepsilon^+ = 0.087$, is near the lower allowed range and can be considered a good compromise.

In this work a food-grade rubber pipe reinforced with two spring steel helices in the thickness and manufactured on a chromium-plated mandrel has been selected. The manufacturing process guarantees a very good surface finishing and spring steel helices guarantee from section deformations. Internal wall waves and irregularities are well below the previously estimated limits. The pipe has an internal diameter of 102 mm, it is 40 m long and has been wrapped on a steel cylinder with a 0.9 m external diameter. The number of wraps is 12.5 and they are kept as close as possible in order to reproduce a nearly toroidal geometry. The measurement will be performed at the beginning of the last wrap, more than 350 diameters after the pump, to be sure that turbulence and Dean flow is fully developed in the test section. A sketch of the complete setup and a photograph of the coil is reported in Figure 2. In Table 1 values assumed by the main parameters in the present setup are reported.

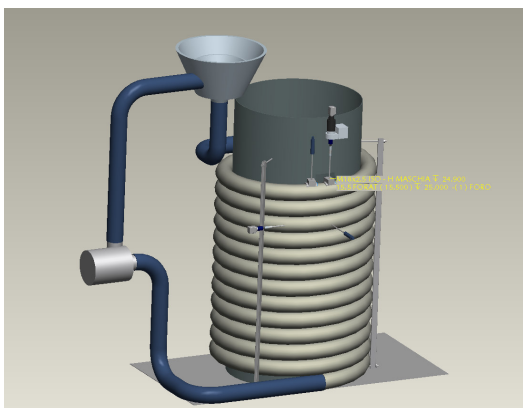


Figure 2. Complete setup of the coil and the real pipe

Table 1. Geometrical and flow properties for the actual coil configuration

Geometrical properties		Water flow properties	
Internal pipe diameter [mm]	102	Bulk velocity [m/s]	0.11
Pipe thickness [mm]	8	Mass flow rate [kg/s]	0.91
Coil internal diameter [mm]	900	Reynolds number	10000
Coil centreline diameter [mm]	1018	Dean number	3165
Coil height [mm]	1475	Germano number	$3.7 \cdot 10^{-6}$
Pitch [mm]	118	Torsion to curvature ratio	0.037
Wraps	12.5	Kinematic viscosity [m ² /s]	$1.14 \cdot 10^{-6}$
Curvature ratio	0.1	Density [kg/m ³]	999.1

The water flow is provided by a centrifugal pump. The flow is passed through a honeycomb flow-straightener to suppress the flow swirl due to the pump. A standard orifice is employed as flow-meter.

3. The PIV system

The PIV system is based on a 2W continuous argon laser light source and on a PIV camera equipped with a light intensifier.

The laser wavelength is 514.5 nm (green light) which is transmitted by water very well. In order to allow the endoscopic investigation a rigid boroscope and an endoscopic illuminator are employed. The former is coupled with the intensifier by means of an appropriate adaptor, the latter produces the laser sheet inside the investigation area and is coupled with the laser light source. Both endoscopic instruments (the scope and the illuminator) have an 8mm diameter and can be equipped with a 45° mirror to produce a 90° degrees deflection of vision or illumination direction, as can be seen in Figure 3. A general scheme of the system is sketched in Figure 4.

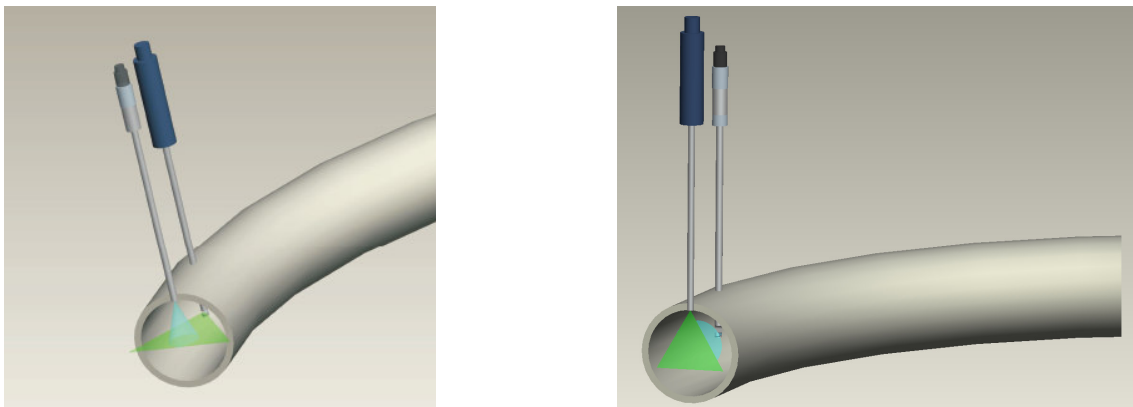


Figure 3. Sketch of the light sheet and vision endoscope set-up

3.1 The light intensifier

Owing to the small aperture of the boroscope, whose lens diameter is just 3 mm, a very small quantity of light can be captured by the optics, roughly two orders of magnitude less than with standard lenses. For this reason, two different solutions, a high energy pulsed laser source or an image intensifier unit, can be adopted. In this work the use of an image intensifier has been preferred, since gains order of 10^3 are usually achieved by commercial units, a factor which is difficult to obtain for laser sources. It should be noted also that, owing to the low velocities to be measured, quite high exposure times are feasible, so that the energy provided by a continuous laser is just an order of magnitude lower than that provided by a low energy pulsed laser source.

A Hamamatsu C9548-03 image intensifier unit has been selected. This model has been developed to support high speed cameras. It is capable of a minimum gate time of 10 ns and a maximum gate repetition rate of 200kHz. In burst mode, it

is able to produce up to 16 exposures with a delay time between them of 500 ns, which is comparable to double shutter cameras interframe time.

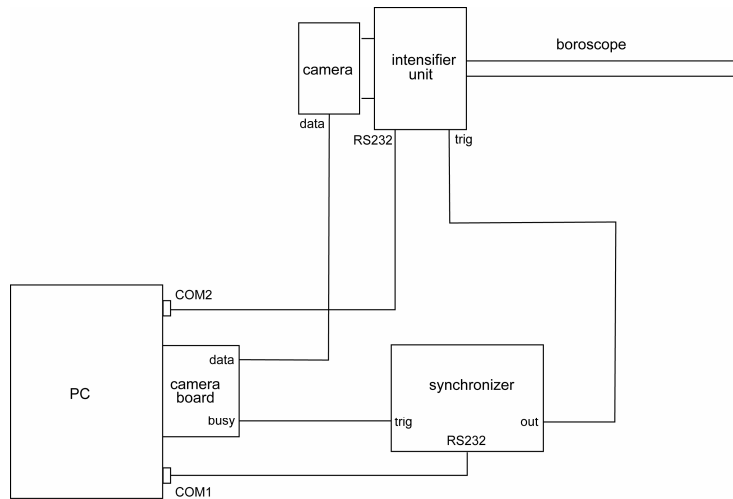


Figure 4. Frame acquiring system scheme

The image intensifier unit has a synthetic quartz photocathode window and a multi-alkaline photocathode, so that its spectral response curve is particularly wide, ranging from 200 nm up to 800nm. The photocathode diameter is 25 mm and its resolution is 57 line pairs per millimetre MTF at 5%, which means a resolution approximately equivalent to that of a 1600 x 1200 pixel camera, when the camera CCD is perfectly mapped to the photocathode, see Figure 5. This means that no resolution penalization follows from the use of the intensifier, since the employed camera has a resolution of 1280 x 1024 pixel.

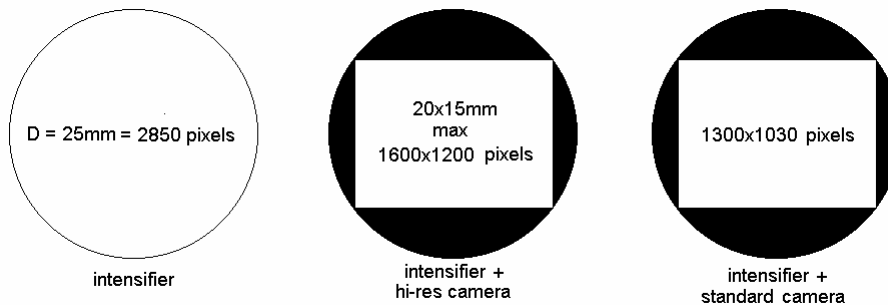


Figure 5. Photocathode resolution and CCD mapping

3.2 The seeding

One of the main problems when PIV is applied to flows in internal ducts, and in particular when measurements close to the duct walls are required, is the effect of light reflection on the duct wall. Reflections can also be dangerous for the instrumentation, and in particular for the image intensifier unit that could be damaged from a direct exposition to the laser source or to a reflection. Among the measurement techniques available to solve the problem, fluorescent particles are an ideal solution for PIV measurements in water when used in conjunction with a sharp band-pass filter: in fact they enhance the signal to noise ratio and eliminate all reflections from walls, air bubbles or other impurities that could be present in water.

Polystyrene particles seem to be most appropriate for our application because their density is 1.05 g/cm^3 , very close to the water density. Red fluorescent, $8 \text{ }\mu\text{m}$ diameter, particles have been selected with an excitation wavelength of 542 nm, green, very close to the emission wavelength of the laser source, and an emission wavelength of 612 nm (red), the excitation and response curve is reported in Figure 6. Owing to the particle cost, a closed loop duct must be necessarily employed not to waste them. The particles have been purchased from Duke Scientific Corporation.

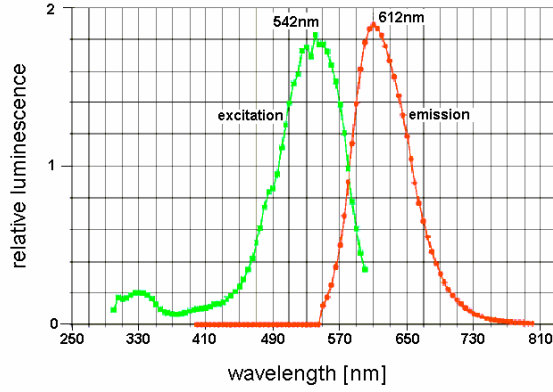


Figure 6. Fluorescent particle response curve (left excitation, right emission)

3.3 Image acquisition

A critical parameter in PIV measurements is the time delay between the two frames to be correlated to obtain velocity vectors. In particular, when secondary flow velocity components are to be measured, a critical parameter is the time t_p that is necessary to a single particle to pass through the laser beam thickness. The time between two consecutive frames must be significantly less than t_p , so that most of the particles that lay inside the light sheet thickness at the time of the first photogram will still be there at the time of the second one, thus making correlations between the two pictures possible. An estimate of t_p based on the bulk velocity U_b and on the light sheet thickness s_l can be readily obtained. In our case, we can roughly assume $s_l = 1$ mm so that

$$t_p = \frac{s_l}{U_b} = \frac{0.001 \text{ m}}{0.11 \text{ m/s}} = 0.009 \text{ s} .$$

To complete the analysis it is necessary to choose the size of the field of view. The choice must accommodate two conflicting requirements: on one hand, the largest possible field of view would be useful, on the other hand, since the camera resolution is fixed, the larger the field of view, the lower the resolution. Moreover, for a fixed time delay between two successive frames, the displacement of the particle, measured in pixels, is lower as the field of view is larger, so that the accuracy of the computed velocity is lower as the field grows.

4. Data reduction and accuracy of the system

The images acquired by the digital camera are processed by means of a software developed by the authors following Raffel et al.¹³. In order to obtain a better accuracy, the classical three point subpixel interpolation is applied. This is rather important in the present work as a focus point is the description of the secondary flow that is characterized by very small velocities, compared to bulk velocity U_b . Taking a typical secondary velocity magnitude order of $0.1 U_b$ (as it is expected⁹) and a light sheet thickness of about 1mm and considering that the time delay between two successive frames should not exceed one fourth of the time that a particle spends to cross over the light sheet, the typical displacement that has to be measured is order of 0.025 mm. Considering a 31mm x 25mm field of view and taking into account that adopted camera has a 1280x1024 resolution, a pixel roughly corresponds to 0.024mm and thus the typical measured displacement corresponds to one pixel. As the subpixel interpolation allows an accuracy of 1/10th to 1/20th of a pixel, the error should not exceed 10%, and can be considered acceptable for the aim of the present work. Nevertheless an higher accuracy would certainly be appreciated and therefore more accurate methods will be implemented in the frame processing program applying more recent methods available in the literature^{20,21}.

5. System pre-test

Some preliminary tests of the optical system have been carried out in order to verify that the system is working correctly. Particle images of a simple water flow have been acquired inside a closed tank (see Figure 7). The tests show that particles, white polystyrene particles have been used for the test, are clearly visible and that, generally speaking, the system is working correctly.



Figure 7. Example of a frame acquired by the proposed system

6. Conclusions

A new experimental facility for the study of curved pipe turbulent flows has been designed and set up at Dipartimento di Ingegneria Aerospaziale, Politecnico di Milano. It consists of a tube helically coiled on a steel core. The facility allows for several investigations on curvature effects on turbulent flow structure. All design parameters have been defined in detail. Particular care has been devoted to the choice of the pipe, and in particular to the internal surface finishing in order to prevent any undesirable perturbation on the secondary flow structures to be observed. Roughness and wall wave dimension have been checked to be in the allowed range. The optical measurement system (endoscopic PIV) has been developed and pre-tested and it is now ready to be used. This new facility is now available for a wide campaign of experimental investigations.

References

- [1] Berger S. A., Talbot L., Yao L. S., "Flow in curved pipes", *Ann. Rev. Fluid Mech.* 15, pp. 461-512, 1983.
- [2] Vasudevaiah M., Patturaj R., "Effect of Torsion in an Helical Pipe Flow", *Internat. J. Math. & Math. Sci.* 17, pp. 553-560, 1994.
- [3] Zabielski L., Mestel A. J., "Steady flow in a helically symmetric pipe", *J. Fluid Mech.* 370, pp. 297-320, 1998.
- [4] Hüttl T. J., Wagner C., Friedrich R., "Navier-Stokes solutions of laminar flows based on orthogonal helical coordinates", *Int. J. Numer. Meth. Fluids* 29, pp. 749-763, 1999.
- [5] Fan Y., Tanner R. I., Phan-Thien N., "Fully developed viscous and viscoelastic flows in curved pipes", *J. Fluid Mech.* 440, pp. 327-357, 2001.
- [6] Webster D.R., Humphrey J.A.C., "Experimental Observations of Flow Instability in a Helical Coil", *J. Fluids Eng.* 115, pp.436-443, 1993.
- [7] Webster D. R., Humphrey J. A. C., "Traveling wave instability in helical coil flow", *Phys. Fluids* 9, pp. 407-418, 1997.
- [8] Lin C. X., Ebdian M. A., "The effects of inlet turbulence on the development of fluid flow and heat transfer in a helically coiled pipe", *Int. J. Heat Mass Tran.* 42, pp. 739-751, 1999.
- [9] Hüttl T.J., Friedrich R., "Direct numerical simulation of turbulent flows in curved and helically coiled pipes", *Computers & Fluids* 30, 2001, p.591-605.
- [10] Ligrani P.M., Niver R.D., "Flow visualization of Dean vortices in a curved channel with 40 to 1 aspect ratio", *Phys. Fluids* 31, pp.3605-3617, 1988.
- [11] Yamamoto K., Wu X., Nozaki K., Hayamizu Y., "Visualization of Taylor-Dean flow in a curved duct of square cross section", *Fluid Dynamics Research* 38, pp. 1-18, 2006.
- [12] Srinivasan P.S., Nandapurkar S., Holland F.A., "Friction factors for coil", *Tran. Inst. Chem. Eng.* 48, pp. 156-161, 1970.
- [13] M. Raffel, C. E. Willert, J. Kompenhans, *Particle image velocimetry: a practical guide*, Springer 1998.
- [14] Xiong W., Merzkirch W., "PIV experiments using an endoscope for studying pipe flow", *J. Flow Vis. Image Proc.* 6, pp. 167-175, 1999.

- [15] Gratton M.B., "The effects of torsion on Anomalous Diffusion in Helical Pipe", Harvey Mudd College, pp. 43, 2002
- [16] Germano M., "On the effect of torsion on a helical pipe flow", J. Fluid Mech. 125, pp. 1-8, 1982.
- [17] Germano M., "The Dean equations extended to a helical pipe flow", J. Fluid Mech. 203, pp. 289-305, 1989.
- [18] Nakagawa S., Hanratty T. J., "Particle image velocimetry measurements of flow over a wavy wall", Phys. Fluids 13, pp. 3504-3507, 2001.
- [19] Quadrio M., Sibilla S., "Numerical simulation of turbulent flow in a pipe oscillating around its axis", J. Fluid Mech. 424, pp. 217-241, 2000.
- [20] Roesgen T., "Optimal subpixel interpolation in particle image velocimetry", Exp. in Fluids 35, pp. 252-256, 2004.
- [21] Nobach H., Damaschke N., Tropea C., High-precision sub-pixel interpolation in particle image velocimetry image processing", Exp. in Fluids 39, pp. 299-304, 2005.